Eur. Phys. J. C (2021) 81:1108
https://doi.org/10.1140/epjc/s10052-021-09916-w

THE EUROPEAN PHYSICAL JOURNAL C

Regular Article - Theoretical Physics

Strange hidden-charm tetraquarks in constituent quark model

Xin Jin[1,a], **Yuheng Wu**[1,b], **Xuejie Liu**[2,c], **Hongxia Huang**[1,d], **Jialun Ping**[1,e], **Bin Zhong**[1,f]

[1] Department of Physics, Nanjing Normal University, Nanjing 210023, People's Republic of China
[2] School of Physics, Southeast University, Nanjing 210094, People's Republic of China

Received: 12 August 2021 / Accepted: 6 December 2021 / Published online: 15 December 2021

Abstract In the framework of the chiral quark model (ChQM), we systematically investigate the strange hidden-charm tetraquark systems $cs\bar{c}\bar{u}$ with two structures: $q\bar{q}-q\bar{q}$ and $qq-\bar{q}\bar{q}$. The bound-state calculation shows that there is no any bound state in present work, which excludes the molecular state explanation ($D^0D_s^{*-}/D^{*0}D_s^-/D^{*0}D_s^{*-}$) of the reported $Z_{cs}(3985)^-$ or $Z_{cs}(4000)^+$. However, the effective potentials for the $cs-\bar{c}\bar{u}$ systems show the possibility of some resonance states. By applying a stabilization calculation and coupling all channels of both two structures, two new resonance states are obtained, which are the $IJ^P=\frac{1}{2}0^+$ state with the energy around 4111–4116 MeV and the $IJ^P=\frac{1}{2}1^+$ state with energy around 4113–4119 MeV, respectively. Both of them are worthy of search in future experiments. Our results show that the coupling calculation between the bound channels and open channels is indispensable to provide the necessary information for experiments to search for exotic hadron states.

1 Introduction

In 2013, the BESIII Collaboration reported a new charged charmonium-like structure in the $\pi^\pm J/\psi$ invariant spectrum, which is called $Z_c(3900)$ [1]. At the same time, the Belle observed a $Z_c(3895)^\pm$ state in the process $Y(4260)\to J/\psi\pi^+\pi^-$ [2]. The mass and width of $Z_c(3900)$ and $Z_c(3895)^\pm$ are very close within errors, so they are the same state [3]. Subsequently, a series of the Z_c exotic resonances have been reported experimentally, such as $Z_c(4020)$ [4], $Z_c^\pm(4025)$ [5], $Z_c(3885)^-$ [6], $Z_c(4200)^+$ [7] and $Z_c(4025)^0$ [8].

In the last year, the BESIII Collaboration reported their study of the processes of $e^+e^-\to K^+(D_s^-D^{*0}+D_s^{*-}D^0)$, and found a new structure $Z_{cs}(3985)^-$ near the $D_s^-D^{*0}/D_s^{*-}D^0$ thresholds. The pole mass and width of this state are $(3982.5^{+1.8}_{-2.6}\pm 2.1)$ Mev and $(12.8^{+5.3}_{-4.4}\pm 3.0)$ Mev, respectively [9]. From the production mode, it is easy to get that the minimum quark component of $Z_{cs}(3985)^-$ is $cs\bar{c}\bar{u}$, and this state should be a partner structure of the well-known $Z_c(3885)^-$ reported in $e^+e^-\to D^{*-}D^0\pi^+$ [6]. Besides, it is the first candidate of the charged hidden-charm tetraquark state with strangeness, whose discovery can provide more hints to the quest of charged exotic Z structures. Therefore, the observation of $Z_{cs}(3985)^-$ immediately stimulated a lot of theoretical discussions [10–24].

Recently, the LHCb Collaboration observed the $Z_{cs}(4000)^+$ and $Z_{cs}(4220)^+$ with a new quark content $cu\bar{c}\bar{s}$ decaying to the $J/\psi K^+$ final state [25], and the decay widths of these two states are $\Gamma=131\pm 15\pm 26$ MeV and $\Gamma=233\pm 52^{+97}_{-73}$ MeV, respectively. The masses of $Z_{cs}(3985)^-$ and $Z_{cs}(4000)^+$ are very close, but the decay widths are very different, so there are a lot of theoretical works to study Z_{cs} states. Some theorists obtained that $Z_{cs}(3985)^-$ and $Z_{cs}(4000)^+$ are the same state [26,27]. In addition, some people showed that they are not the same state and give separate explanations [12,28–30]. While discussing these states, many theoretical workers also found new states in system of $cs\bar{c}\bar{u}$. In Ref. [14], they made a prediction of the missing kaon spectrum for the potential $Z_{cs}(4120)$ as a hadronic molecule of $\bar{D}_s^*D^*$. In Ref. [26], they predicted a new state $Z_{cs}(4110)^-$ which is the $SU(3)_f$ partner of $Z_c(4020)^+$ by Chiral constituent quark model. In Ref. [28], they predicted some possible tetraquark states by use of an effective Hamiltonian. The values of two model parameters are 4141 MeV and 4095 MeV for $J^P=0^+$ respectively, 4163 MeV and 4117 MeV for $J^P=1^+$, 4185 MeV and 4231 MeV for $J^P=2^+$. In Ref. [29], a tensor $\bar{D}_s^*D^*$ res-

[a] e-mail: 181002005@njnu.edu.cn
[b] e-mail: 191002007@njnu.edu.cn
[c] e-mail: 1830592517@qq.com
[d] e-mail: hxhuang@njnu.edu.cn (corresponding author)
[e] e-mail: jlping@njnu.edu.cn (corresponding author)
[f] e-mail: zhongb@njnu.edu.cn

onance with mass about 4126 MeV and width 13 MeV was obtained within a nonrelativistic effective field theory. In Ref. [20], they found a new state, $Z_{cs}(4125)$, in the $\bar{D}_s^* D^*$ system, which can be strange partner of $Z_c(4020)^+$ state.

Actually, theoretical predictions of the charged hidden-charm tetraquark with strangeness have been made in different models [31–33]. D.Ebert used relativistic quark model based on the quasipotential approach to calculate the mass spectra of tetraquarks $[Qs][\bar{Q}\bar{q}]/[Qq][\bar{Q}\bar{s}](Q = c, b)$ [34]. They found that all S-wave tetraquarks with hidden bottom lie considerably below open bottom thresholds and they should be narrow states which can be observed experimentally. However hidden-charm tetraquark states all above open charm thresholds. Dianyong Chen indicated that there exist enhancement structures with both hidden-charm and open-strange decays, which are near the $D\bar{D}_s^*/D^*\bar{D}_s$ and $D^*\bar{D}_s^*/\bar{D}^* D_s^*$ thresholds under the initial single chiral particle emission (ISChE) mechanism [35]. Chengrong Deng studied the same charged tetraquark states using the variational method GEM in the color flux-tube model with a four-body confinement potential. The numerical results indicated that some compact resonance states can be formed [36].

Strong interaction is the strongest one of the four interactions in nature, but understanding its nature has always been a difficult problem in physics. Quantum chromodynamics (QCD) is widely accepted as the basic theory of strong interactions. QCD can deal with scattering problems by perturbation expansion in high energy regions, but the spontaneous chiral symmetry breaking and color confinement appear in low energy regions. To study hadron–hadron interactions and multiquark states, many quark models based on QCD theory have been developed. The chiral quark model (ChQM) is one of the typical models [37]. The interactions in this model include the colorful one-gluon-exchange and confinement, colorless Goldstone boson exchange and the chiral partner σ meson-exchange. Recently, ChQM has been applied to the study of the fully heavy tetraquark systems [38] and the reported $X(6900)$ [39] was explained as a compact resonance state in this model. It is quite natural to extend the study to the charged hidden-charm tetraquark systems with strangeness. On the one hand, we want to investigate the reported Z_{cs} states. On the other hand, we also try to search for other possible exotic states.

The structure of this paper is as follows. Section 2 gives a brief introduction of ChQM, and the construction of wave functions. The numerical results and discussions are given in Sect. 3. The summary is presented in the last section.

2 Quark model and calculation method

In this work, we investigate the charged charmonium-like tetraquarks with hidden-charm and open-strange $cs\bar{c}\bar{u}$ within ChQM. Two structures: $q\bar{q}-q\bar{q}$ and $qq-\bar{q}\bar{q}$, are considered. In this sector, we will introduce this model and the wave functions of the tetraquarks for two structures.

2.1 Quark model

The ChQM has been successfully applied to describe the properties of hadrons and hadron–hadron interactions [37, 40]. The model details can be found in Refs. [37,40]. The Hamiltonian of this model is:

$$H = \sum_{i=1}^{4}\left(m_i + \frac{p_i^2}{2m_i}\right) - T_{cm} + \sum_{i<j=1}^{4}(V_{ij}^{CON} + V_{ij}^{OGE}) \tag{1}$$

where T_{cm} is the kinetic energy of the center of mass; V_{ij}^{CON} and V_{ij}^{OGE} are the interactions of the confinement and the one-gluon-exchange, respectively. For the $cs\bar{c}\bar{u}$ system, there is no σ-exchange interactions, because the σ meson cannot be exchanged between u/d quark and s/c quark. The forms of V_{ij}^{CON} and V_{ij}^{OGE} are shown below:

$$V_{ij}^{CON} = -\boldsymbol{\lambda}_i^c \cdot \boldsymbol{\lambda}_j^c (a_c r_{ij}^2 + V_{0_{q_i q_j}}) \tag{2}$$

$$V_{ij}^{OGE} = \frac{\alpha_{s_{q_i q_j}}}{4}\boldsymbol{\lambda}_i^c \cdot \boldsymbol{\lambda}_j^c \left[\frac{1}{r_{ij}} - \frac{\pi}{2}\delta(\mathbf{r}_{ij})\left(\frac{1}{m_i^2} + \frac{1}{m_j^2} + \frac{4\boldsymbol{\sigma}_i \cdot \boldsymbol{\sigma}_j}{3m_i m_j}\right) - \frac{3}{4m_i m_j r_{ij}^3} S_{ij}\right] \tag{3}$$

$$S_{ij} = \left\{3\frac{(\boldsymbol{\sigma}_i \cdot \boldsymbol{r}_{ij})(\boldsymbol{\sigma}_j \cdot \boldsymbol{r}_{ij})}{r_{ij}^2} - \boldsymbol{\sigma}_i \cdot \boldsymbol{\sigma}_j\right\} \tag{4}$$

where S_{ij} is quark tensor operator; $\alpha_{s_{q_i q_j}}$ is the quark–gluon coupling constant.

2.2 Calculation method

We use the resonating group method (RGM) [41] to carry out a dynamical calculation. Following the nomenclature of Ref. [42], we write the conventional ansatz for the two-cluster (cluster A and B) wave function as

$$\Psi_{4q} = \mathcal{A}\sum_L \left[[\Psi_A \Psi_B]^{[\sigma]IS} \bigotimes \chi_L(\mathbf{R})\right]^J. \tag{5}$$

The symbol $\mathcal{A}$ is the anti-symmetrization operator. For the $cs\bar{c}\bar{u}$ system, $\mathcal{A} = 1$ because the quarks are not identical particles in the $SU(3)$ symmetry and no anti-symmetrization requirement is needed here. $[\sigma] = [222]$ gives the total color symmetry and all other symbols have their usual meanings. Ψ_A and Ψ_B are the 2-quark cluster wave functions(after removal of the center of mass motion):

$$\Psi_A = \left(\frac{1}{2\pi b^2}\right)^{3/4} e^{-\boldsymbol{\rho}_\mathbf{A}^2/(4b^2)} \eta_{I_A S_A} \chi_A^c, \tag{6}$$

$$\Psi_B = \left(\frac{1}{2\pi b^2}\right)^{3/4} e^{-\boldsymbol{\rho}_\mathbf{B}^2/(4b^2)} \eta_{I_B S_B} \chi_B^c, \tag{7}$$

where $\eta_{I_A S_A}/\eta_{I_B S_B}$ are the multiplied wave functions of flavor and spin of the cluster A/B; χ_A^c/χ_B^c are the internal color wave functions of cluster A/B, and the Jacobi coordinates are defined as follows:

$$\begin{aligned}
&\boldsymbol{\rho}_\mathbf{A} = \mathbf{r_1} - \mathbf{r_2}, \quad \boldsymbol{\rho}_\mathbf{B} = \mathbf{r_3} - \mathbf{r_4},\\
&\mathbf{R_A} = \frac{1}{2}(\mathbf{r_1} + \mathbf{r_2}), \quad \mathbf{R_B} = \frac{1}{2}(\mathbf{r_3} + \mathbf{r_4}),\\
&\mathbf{R} = \mathbf{R}_A - \mathbf{R}_B, \quad \mathbf{R_C} = \frac{1}{2}(\mathbf{R}_A + \mathbf{R}_B).
\end{aligned} \tag{8}$$

From the variational principle, after variation with respect to the relative motion wave function $\chi(\mathbf{R}) = \sum_L \chi_L(\mathbf{R})$, one obtains the RGM equation

$$\int H(\mathbf{R}, \mathbf{R}')\chi(\mathbf{R}')d\mathbf{R}' = E \int N(\mathbf{R}, \mathbf{R}')\chi(\mathbf{R}')d\mathbf{R}', \tag{9}$$

where $H(\mathbf{R}, \mathbf{R}')$ and $N(\mathbf{R}, \mathbf{R}')$ are Hamiltonian and norm kernels, respectively. Their detailed expressions can be found in Ref. [42]. The energies E and the wave functions are obtained by solving the RGM equation. In practice, it is not convenient to work with the RGM expressions. Then, the relative motion wave function $\chi(\mathbf{R})$ is expanded by gaussian bases

$$\begin{aligned}
\chi(\mathbf{R}) = \frac{1}{\sqrt{4\pi}} \sum_L \left(\frac{1}{\pi b^2}\right)^{3/4} \sum_i C_{i,L}\\
\times \int e^{-\frac{1}{2}(\mathbf{R}-\mathbf{S}_i)^2/b^2} Y^L(\hat{\mathbf{S}}_\mathbf{i}) d\Omega_{S_i},
\end{aligned} \tag{10}$$

where $\mathbf{S_i}$ is the generator coordinate in the model, denoting the separation of two reference centers. $\mathbf{R}$ is the dynamic coordinate defined in Eq. (8). In each cluster, the reference center is fixed, and the quarks move around the reference center, whereas the dynamic coordinate $\mathbf{R}$ is a quantity varies with the motion of each quark. In the right side of Eq. (10), the angular part of $\mathbf{S_i}$ is integrated out, and the sum is over i, so the magnitude of $\mathbf{S_i}$ is also integrated out. So the left side of Eq. (10) only depends on $\mathbf{R}$. $C_{i,L}$ is the expansion coefficient. After the inclusion of the center of mass motion,

$$\Phi_C(\mathbf{R_C}) = \left(\frac{4}{\pi b^2}\right)^{3/4} e^{-2\mathbf{R}_C^2/b^2}, \tag{11}$$

the ansatz, Eq. (5), can be rewritten as

$$\begin{aligned}
\Psi_{4q} = \mathcal{A} \sum_{i,L} C_{i,L} \int \frac{d\Omega_{S_i}}{\sqrt{4\pi}} \prod_{\alpha=1}^{2} \phi_\alpha(\mathbf{S_i}) \prod_{\beta=3}^{4} \phi_\beta(-\mathbf{S_i})\\
\times [[\eta_{I_A S_A} \eta_{I_B S_B}]^{IS} Y^L(\hat{\mathbf{S}}_\mathbf{i})]^J [\chi_A^c \chi_B^c]^{[\sigma]},
\end{aligned} \tag{12}$$

where $\phi_\alpha(\mathbf{S_i})$ and $\phi_\beta(-\mathbf{S_i})$ are the single-particle orbital wave functions with different reference centers:

$$\begin{aligned}
\phi_\alpha(\mathbf{S_i}) &= \left(\frac{1}{\pi b^2}\right)^{3/4} e^{-\frac{1}{2}(\mathbf{r_\alpha} - \mathbf{S_i}/2)^2/b^2},\\
\phi_\beta(-\mathbf{S_i}) &= \left(\frac{1}{\pi b^2}\right)^{3/4} e^{-\frac{1}{2}(\mathbf{r_\beta} + \mathbf{S_i}/2)^2/b^2}.
\end{aligned} \tag{13}$$

With the reformulated ansatz, Eq. (12), the RGM equation (9) becomes an algebraic eigenvalue equation:

$$\sum_{j,L} C_{j,L} H_{i,j}^{L,L'} = E \sum_j C_{j,L'} N_{i,j}^{L'}, \tag{14}$$

where $N_{i,j}^{L'}$ and $H_{i,j}^{L,L'}$ are the wave function (12) overlaps and Hamiltonian matrix elements (without the summation over L'), respectively. By solving the generalized eigen problem, we can obtain the energies of the 4-quark systems E and corresponding expansion coefficient $C_{j,L}$. Finally, the relative motion wave function between two clusters can be obtained by substituting the $C_{j,L}$ into Eq. (10). The flavor, spin and color wave functions are constructed in the following part.

2.2.1 The flavor wave function

In this work, the flavor wave function for the tetraquark system we investigate is $cs\bar{c}\bar{u}$. Different structures are obtained according to different coupling sequences. For the $q\bar{q} - q\bar{q}$ structure, we use two kinds of coupling sequence, which are

$$\chi_m^{f1} = c\bar{c} - s\bar{u} \tag{15}$$

$$\chi_m^{f2} = c\bar{u} - s\bar{c}. \tag{16}$$

For the $qq - \bar{q}\bar{q}$ structure, the coupling sequence is

$$\chi_d^{f1} = cs - \bar{c}\bar{u}. \tag{17}$$

Note that this coupling sequence should match the orbital coupling sequence. For the coupling sequence $c\bar{c} - s\bar{u}$, the orbital coordinates are defined as Eq. (8); for the coupling sequence $c\bar{u} - s\bar{c}$, the orbital coordinates in Eq. (8) change to

$$\begin{aligned}
&\boldsymbol{\rho}_\mathbf{A} = \mathbf{r_1} - \mathbf{r_4}, \quad \boldsymbol{\rho}_\mathbf{B} = \mathbf{r_3} - \mathbf{r_2},\\
&\mathbf{R_A} = \frac{1}{2}(\mathbf{r_1} + \mathbf{r_4}), \quad \mathbf{R_B} = \frac{1}{2}(\mathbf{r_3} + \mathbf{r_2}),
\end{aligned} \tag{18}$$

and for the coupling sequence $cs-\bar{c}\bar{u}$, the orbital coordinates in Eq. (8) change to

$$\boldsymbol{\rho}_{\mathbf{A}}=\mathbf{r_1}-\mathbf{r_3},\quad \boldsymbol{\rho}_{\mathbf{B}}=\mathbf{r_2}-\mathbf{r_4},$$
$$\mathbf{R_A}=\frac{1}{2}(\mathbf{r_1}+\mathbf{r_3}),\quad \mathbf{R_B}=\frac{1}{2}(\mathbf{r_2}+\mathbf{r_4}). \tag{19}$$

2.2.2 The spin wave function

For the spin part, the wave functions for two-body clusters are:

$$\chi^1_{\sigma 11}=\alpha\alpha\quad \chi^2_{\sigma 10}=\sqrt{\frac{1}{2}}(\alpha\beta+\beta\alpha)$$
$$\chi^3_{\sigma 1-1}=\beta\beta\quad \chi^4_{\sigma 00}=\sqrt{\frac{1}{2}}(\alpha\beta-\beta\alpha) \tag{20}$$

where the α and β represent spin up $(S, S_z)=(\frac{1}{2}, \frac{1}{2})$ and spin down $(S, S_z)=(\frac{1}{2}, -\frac{1}{2})$, respectively. Then, the total spin wave functions for the four-quark system can be obtained by coupling the wave functions of two clusters.

$$\begin{aligned}
\chi^{\sigma 1}_{00}&=\chi^4_{\sigma 00}\chi^4_{\sigma 00}\\
\chi^{\sigma 2}_{00}&=\sqrt{\frac{1}{3}}(\chi^1_{\sigma 11}\chi^3_{\sigma 1-1}-\chi^2_{\sigma 10}\chi^2_{\sigma 10}+\chi^3_{\sigma 1-1}\chi^1_{\sigma 10})\\
\chi^{\sigma 3}_{11}&=\chi^4_{\sigma 00}\chi^1_{\sigma 11}\\
\chi^{\sigma 4}_{11}&=\chi^1_{\sigma 11}\chi^4_{\sigma 00}\\
\chi^{\sigma 5}_{11}&=\sqrt{\frac{1}{2}}(\chi^1_{\sigma 11}\chi^2_{\sigma 10}-\chi^2_{\sigma 10}\chi^1_{\sigma 11})\\
\chi^{\sigma 6}_{22}&=\chi^1_{\sigma 11}\chi^1_{\sigma 11}.
\end{aligned} \tag{21}$$

The spin wave function of two structures is the same.

2.2.3 The color wave function

For the $q\bar{q}-q\bar{q}$ structure, we give the wave functions for the two-body clusters first, which are

$$\chi^1_{c[111]}=\sqrt{\frac{1}{3}}(r\bar{r}+g\bar{g}+b\bar{b}) \tag{22}$$

$$\begin{aligned}
\chi^2_{c[21]}&=r\bar{b}\quad \chi^3_{c[21]}=-r\bar{g}\\
\chi^4_{c[21]}&=g\bar{b}\quad \chi^5_{c[21]}=-b\bar{g}\\
\chi^6_{c[21]}&=g\bar{r}\quad \chi^7_{c[21]}=b\bar{r}\\
\chi^8_{c[21]}&=\sqrt{\frac{1}{2}}(r\bar{r}-g\bar{g})\\
\chi^9_{c[21]}&=\sqrt{\frac{1}{6}}(-r\bar{r}-g\bar{g}+2b\bar{b})
\end{aligned} \tag{23}$$

where the subscript [111] and [21] stand for the color singlet and color octet cluster respectively.

Then, the total color wave functions for the four-quark system with the $q\bar{q}-q\bar{q}$ structure can be obtained by coupling the wave functions of two clusters.

$$\chi^{c1}_m=\chi^1_{c[111]}\chi^1_{c[111]} \tag{24}$$

$$\begin{aligned}
\chi^{c2}_m=&\sqrt{\frac{1}{8}}(\chi^2_{c[21]}\chi^7_{c[21]}-\chi^4_{c[21]}\chi^5_{c[21]}-\chi^3_{c[21]}\chi^6_{c[21]}\\
&+\chi^8_{c[21]}\chi^8_{c[21]}-\chi^6_{c[21]}\chi^3_{c[21]}+\chi^9_{c[21]}\chi^9_{c[21]}\\
&-\chi^5_{c[21]}\chi^4_{c[21]}+\chi^7_{c[21]}\chi^2_{c[21]})
\end{aligned} \tag{25}$$

where χ^{c1}_m and χ^{c2}_m represent the color wave function for the color-singlet channel (1×1) and the hidden-color channel (8×8), respectively.

For the $qq-\bar{q}\bar{q}$ structure, we firstly give the color wave functions of the diquark clusters,

$$\begin{aligned}
&\chi^1_{c[2]}=rr\quad \chi^2_{c[2]}=\sqrt{\frac{1}{2}}(rg+gr)\quad \chi^3_{c[2]}=gg\\
&\chi^4_{c[2]}=\sqrt{\frac{1}{2}}(rb+br)\quad \chi^5_{c[2]}=\sqrt{\frac{1}{2}}(gb+bg)\\
&\chi^6_{c[2]}=bb\quad \chi^7_{c[11]}=\sqrt{\frac{1}{2}}(rg-gr)\\
&\chi^8_{c[11]}=\sqrt{\frac{1}{2}}(rb-br)\quad \chi^9_{c[11]}=\sqrt{\frac{1}{2}}(gb-bg)
\end{aligned} \tag{26}$$

and the color wave functions of the antidiquark clusters,

$$\begin{aligned}
&\chi^1_{c[22]}=\bar{r}\bar{r}\quad \chi^2_{c[22]}=\sqrt{\frac{1}{2}}(\bar{r}\bar{g}+\bar{g}\bar{r})\quad \chi^3_{c[22]}=\bar{g}\bar{g}\\
&\chi^4_{c[22]}=\sqrt{\frac{1}{2}}(\bar{r}\bar{b}+\bar{b}\bar{r})\quad \chi^5_{c[22]}=\sqrt{\frac{1}{2}}(\bar{g}\bar{b}+\bar{b}\bar{g})\\
&\chi^6_{c[22]}=\bar{b}\bar{b}\quad \chi^7_{c[211]}=\sqrt{\frac{1}{2}}(\bar{r}\bar{g}-\bar{g}\bar{r})\\
&\chi^8_{c[211]}=\sqrt{\frac{1}{2}}(\bar{r}\bar{b}-\bar{b}\bar{r})\quad \chi^9_{c[211]}=\sqrt{\frac{1}{2}}(\bar{g}\bar{b}-\bar{b}\bar{g}).
\end{aligned} \tag{27}$$

After that, the total wave functions for the four-quark system with the $qq-\bar{q}\bar{q}$ structure are obtained as below,

$$\begin{aligned}
\chi^{c1}_d=&\sqrt{\frac{1}{6}}[\chi^1_{c[2]}\chi^1_{c[22]}-\chi^2_{c[2]}\chi^2_{c[22]}+\chi^3_{c[2]}\chi^3_{c[22]}\\
&+\chi^4_{c[2]}\chi^4_{c[22]}-\chi^5_{c[2]}\chi^5_{c[22]}+\chi^5_{c[2]}\chi^5_{c[22]}]
\end{aligned} \tag{28}$$

$$\chi^{c2}_d=\sqrt{\frac{1}{3}}[\chi^7_{c[11]}\chi^7_{c[211]}-\chi^8_{c[11]}\chi^8_{c[211]}+\chi^9_{c[11]}\chi^9_{c[211]}]. \tag{29}$$

Finally, we can acquire the total wave functions by substituting the wave functions of the orbital, the spin, the flavor and the color parts into the Eq. (5) according to the given quantum number of the system.

Table 1 Model parameters. We used the same m_u(313 MeV), m_s(536 MeV), m_c(1728 MeV) and a_c(101 MeV fm^{-2}) for the three sets of parameters

	I	II	III
$b(fm)$	0.29	0.3	0.31
$V_{0_{us}}$ (MeV)	−192.0	−180.6	−170.0
$V_{0_{uc}}$ (MeV)	−143.3	−133.6	−124.8
$V_{0_{sc}}$ (MeV)	−76.8	−68.1	−59.2
$V_{0_{cc}}$ (MeV)	61.2	76.0	91.0
$\alpha_{s_{us}}$	0.30	0.33	0.36
$\alpha_{s_{uc}}$	0.34	0.38	0.42
$\alpha_{s_{sc}}$	0.60	0.66	0.73
$\alpha_{s_{cc}}$	1.51	1.67	1.84

Table 2 The calculated masses (in MeV) of the mesons. Experimental values are taken from the Particle Data Group (PDG)

	K	K^*	η_c	J/ψ
Exp.	495.0	892.7	2983.9	3096.9
ChQM I	494.8	894.3	2983.8	3096.8
ChQM II	494.6	891.6	2983.6	3096.5
ChQM III	497.4	889.9	2984.2	3096.9
	D	D^*	D_s	D_s^*
Exp.	1864.8	2006.9	1968.3	2112.2
ChQM I	1866.5	2007.0	1967.3	2112.5
ChQM II	1865.5	2007.3	1968.4	2112.2
ChQM III	1865.0	2007.0	1968.0	2112.2

2.3 Model parameters

In fact, the parameter b appeared in Eqs. (6) and (7) represents the size of the cluster. However, the color-octet cluster is not the real physical state. So the b is determined by fitting the size of the mesons. In this work, eight mesons are used, which are K, K^*, D, D^*, D_s, D_s^*, η_c, and J/ψ. Our group has calculated the mass of these mesons by using the Gaussian expansion method (GEM), and found that the average size of these mesons is about 0.3 fm. So we take the value of b around 0.3 fm here. Besides, the quark mass and the parameter a_c are also taken from the work by the GEM [43]. However, we use the resonating group method (RGM) in this work, the main feature of which is that it assumes that the clusters are frozen inside. So we cannot obtain the same mass of these mesons as the GEM. To obtain the right mass of mesons and keep the thresholds of the tetraquark system correct, the parameters $\alpha_{s_{q_iq_j}}$ and $V_{0_{q_iq_j}}$ are fixed by masses of the corresponding mesons. Take D_s and D_s^* as an example. The parameter $\alpha_{s_{sc}}$ can be obtained by fitting the mass difference between D_s and D_s^*. The parameter $V_{0_{q_iq_j}}$ is determined by fitting the mass shift of the absolute and experimental value of each meson. These parameters are related to the flavor and therefore inevitably increase the number of parameters. In order to test the dependence of the results on the parameters and give ranges of the results, three sets of parameters are used in the calculation, which are listed in Table 1. The calculated masses of the mesons are shown in Table 2.

3 Numerical results and discussions

In this work, we investigate the charged hidden-charm tetraquark systems with strangeness in two structures: $q\bar{q}-q\bar{q}$ and $qq-\bar{q}\bar{q}$. We take into account all the possible quantum numbers for the $S-$wave $cs\bar{c}\bar{u}$ systems, which are $IJ^P = \frac{1}{2}0^+$, $\frac{1}{2}1^+$, and $\frac{1}{2}2^+$. For the $q\bar{q}-q\bar{q}$ structure, we take into account of two color configurations which are the color singlet–singlet (1×1) and color octet–octet (8×8) configurations. For the $qq-\bar{q}\bar{q}$ structure, two color configurations, antitriplet-triplet ($\bar{3}\times3$) and sextet–antisextet ($6\times\bar{6}$), are considered.

To find any bound states of the $cs\bar{c}\bar{u}$ systems, we carry out a dynamical bound-state calculation. The energies of both the single channel and the channel-coupling calculations are obtained. Tables 3 and 4 show the results of the $q\bar{q}-q\bar{q}$ structure and the $qq-\bar{q}\bar{q}$ structure, respectively. In the tables, the column headed with $[\chi^{\sigma_i}\chi^{f_j}\chi^{c_k}]$ denotes the combination in spin, flavor and color degrees of freedom for each channel, respectively. The columns headed with E_{th} denotes the theoretical threshold of each channel and E_{sc} represents the lowest energies in the single channel calculation. For $q\bar{q}-q\bar{q}$ structure, the column "Channel" represents the contents of the channel. The results of coupling with all channels (including color-singlet channels and hidden-color channels) are labeled as E_{cc}. For $qq-\bar{q}\bar{q}$ structure, E_{cc} denotes the lowest energies of the coupling of all channels (including $6\times\bar{6}$ and $\bar{3}\times3$ color configurations). All the general features of the calculated results are as follows.

3.1 $q\bar{q}-q\bar{q}$ structure

For the $q\bar{q}-q\bar{q}$ structure, η_cK^- and $\eta_{c8}K_8^-$ in Table 3 represent the color singlet–singlet (1×1) and color octet–octet (8×8) configurations, respectively. From Table 3 we can see that the energy of every single channel is above the corresponding theoretical threshold. The results of the three sets of parameters also agree with each other. The channel-coupling calculation cannot help too much, and the energies by the channel-coupling are still above the theoretical threshold, which indicates that the effect of the channel-coupling is very small here. This is mainly due to the large energy difference between each single channel. As a result, in the

Table 3 The energies of $cs\bar{c}\bar{u}$ systems with the $q\bar{q}-q\bar{q}$ structure (unit: MeV)

IJ^P	$[\chi^{\sigma_i}\chi^{f_j}\chi^{c_k}]$	Channel	ChQM I			ChQM II			ChQM III		
			E_{th}	E_{sc}	E_{cc}	E_{th}	E_{sc}	E_{cc}	E_{th}	E_{sc}	E_{cc}
$\frac{1}{2}0^+$	$\chi_{00}^{\sigma 1}\chi_m^{f 1}\chi_m^{c1}$	$\eta_c K^-$	3478.6	3485.5	3482.3	3478.2	3484.9	3484.9	3481.6	3488.2	3488.1
	$\chi_{00}^{\sigma 2}\chi_m^{f 1}\chi_m^{c1}$	$J/\psi K^{*-}$	3991.1	3995.3		3988.1	3994.8		3986.8	3993.9	
	$\chi_{00}^{\sigma 1}\chi_m^{f 1}\chi_m^{c2}$	$\eta_{c8}K_8^-$		4484.7			4542.6			4533.6	
	$\chi_{00}^{\sigma 2}\chi_m^{f 1}\chi_m^{c2}$	$J/\psi_8 K_8^{*-}$		4263.2			4363.8			4346.7	
	$\chi_{00}^{\sigma 1}\chi_m^{f 2}\chi_m^{c1}$	$D^0 D_s^-$	3833.8	3839.5		3833.9	3840.6		3833.0	3839.7	
	$\chi_{00}^{\sigma 2}\chi_m^{f 2}\chi_m^{c1}$	$D^{*0}D_s^{*-}$	4119.5	4125.3		4119.5	4126.2		4119.2	4125.9	
	$\chi_{00}^{\sigma 1}\chi_m^{f 2}\chi_m^{c2}$	$D_8^0 D_{s8}^-$		4269.3			4395.5			4375.7	
	$\chi_{00}^{\sigma 2}\chi_m^{f 2}\chi_m^{c2}$	$D_8^{*0}D_{s8}^{*-}$		3920.9			4125.3			4091.2	
$\frac{1}{2}1^+$	$\chi_{11}^{\sigma 3}\chi_m^{f 1}\chi_m^{c1}$	$\eta_c K^{*-}$	3878.1	3884.9	3598.3	3875.2	3881.9	3597.8	3874.1	3880.8	3600.9
	$\chi_{11}^{\sigma 4}\chi_m^{f 1}\chi_m^{c1}$	$J/\psi K^-$	3591.6	3598.3		3591.1	3597.8		3594.3	3601.0	
	$\chi_{11}^{\sigma 5}\chi_m^{f 1}\chi_m^{c1}$	$J/\psi K^{*-}$	3991.1	3997.9		3988.1	3994.8		3986.8	3993.5	
	$\chi_{11}^{\sigma 3}\chi_m^{f 1}\chi_m^{c2}$	$\eta_{c8}K_8^{*-}$		4499.6			4493.0			4484.5	
	$\chi_{11}^{\sigma 4}\chi_m^{f 1}\chi_m^{c2}$	$J/\psi_8 K_8^-$		4535.4			4528.5			4519.5	
	$\chi_{11}^{\sigma 5}\chi_m^{f 1}\chi_m^{c2}$	$J/\psi_8 K_8^{*-}$		4434.2			4423.6			4411.0	
	$\chi_{11}^{\sigma 3}\chi_m^{f 2}\chi_m^{c1}$	$D^0 D_s^{*-}$	3979.0	3985.8		3977.7	3984.4		3977.2	3983.8	
	$\chi_{11}^{\sigma 4}\chi_m^{f 2}\chi_m^{c1}$	$D^{*0}D_s^-$	3974.3	3981.5		3975.7	3982.4		3975.0	3981.7	
	$\chi_{11}^{\sigma 5}\chi_m^{f 2}\chi_m^{c1}$	$D^{*0}D_s^{*-}$	4119.5	4126.2		4119.5	4126.2		4119.2	4125.9	
	$\chi_{11}^{\sigma 3}\chi_m^{f 2}\chi_m^{c2}$	$D_8^0 D_{s8}^{*-}$		4396.4			4377.5			4357.7	
	$\chi_{11}^{\sigma 4}\chi_m^{f 2}\chi_m^{c2}$	$D_8^{*0}D_{s8}^-$		4397.0			4377.7			4357.9	
	$\chi_{11}^{\sigma 5}\chi_m^{f 2}\chi_m^{c2}$	$D_8^{*0}D_{s8}^{*-}$		4273.8			4247.2			4220.3	
$\frac{1}{2}2^+$	$\chi_{11}^{\sigma 6}\chi_m^{f 1}\chi_m^{c1}$	$J/\psi K^{*-}$	3991.1	3997.9	3997.4	3988.1	3994.8	3994.8	3986.8	3993.5	3993.3
	$\chi_{11}^{\sigma 6}\chi_m^{f 1}\chi_m^{c2}$	$J/\psi_8 K_8^{*-}$		4532.5			4529.6			4525.1	
	$\chi_{11}^{\sigma 6}\chi_m^{f 2}\chi_m^{c1}$	$D^{*0}D_s^{*-}$	4119.5	4126.2		4119.5	4126.2		4119.2	4125.9	
	$\chi_{11}^{\sigma 6}\chi_m^{f 2}\chi_m^{c2}$	$D_8^{*0}D_{s8}^{*-}$		4473.9			4462.0			4449.0	

Table 4 The energies of $cs\bar{c}\bar{u}$ systems with the $qq-\bar{q}\bar{q}$ structure (unit: MeV)

IJ^P	$[\chi^{\sigma_i}\chi^{f_j}\chi^{c_k}]$	ChQM I			ChQM II			ChQM III		
		E_{th}	E_{sc}	E_{cc}	E_{th}	E_{sc}	E_{cc}	E_{th}	E_{sc}	E_{cc}
$\frac{1}{2}0^+$	$\chi_{00}^{\sigma 1}\chi_d^{f 1}\chi_d^{c1}$	3478.6	4478.8	4006.0	3478.2	4462.3	3964.6	3481.6	4363.2	3950.6
	$\chi_{00}^{\sigma 2}\chi_d^{f 1}\chi_d^{c1}$		4202.7			4171.6			4119.8	
	$\chi_{00}^{\sigma 1}\chi_d^{f 1}\chi_d^{c2}$		4267.2			4263.3			4185.3	
	$\chi_{00}^{\sigma 2}\chi_d^{f 1}\chi_d^{c2}$		4358.2			4350.1			4254.5	
$\frac{1}{2}1^+$	$\chi_{11}^{\sigma 3}\chi_d^{f 1}\chi_d^{c1}$	3591.6	4443.7	4125.4	3591.1	4426.8	4091.2	3594.3	4409.1	4058.1
	$\chi_{11}^{\sigma 4}\chi_d^{f 1}\chi_d^{c1}$		4442.6			4426.3			4408.6	
	$\chi_{11}^{\sigma 5}\chi_d^{f 1}\chi_d^{c1}$		4309.4			4285.7			4261.0	
	$\chi_{11}^{\sigma 3}\chi_d^{f 1}\chi_d^{c2}$		4337.4			4334.2			4329.8	
	$\chi_{11}^{\sigma 4}\chi_d^{f 1}\chi_d^{c2}$		4339.5			4335.2			4330.9	
	$\chi_{11}^{\sigma 5}\chi_d^{f 1}\chi_d^{c2}$		4385.0			4379.1			4372.8	
$\frac{1}{2}2^+$	$\chi_{11}^{\sigma 6}\chi_d^{f 1}\chi_d^{c1}$	3991.1	4496.4	4423.5	3988.1	4486.5	4418.1	3986.8	4475.3	4411.1
	$\chi_{11}^{\sigma 6}\chi_d^{f 1}\chi_d^{c2}$		4432.7			4431.1			4428.9	

$q\bar{q} - q\bar{q}$ structure, there is no any bound states. So the reported $Z_{cs}(3985)^-$ or $Z_{cs}(4000)^+$ cannot be explained as $D^0 D_s^{*-}/D^{*0} D_s^-/D^{*0} D_s^{*-}$ molecular state in present calculation.

To study the interaction between two $q\bar{q}$ clusters, we carry out the adiabatic calculation of the effective potentials for the $cs\bar{c}\bar{u}$ system. The effective potential between two clusters is defined as $V(S) = E(S) - E(\infty)$, where $E(S)$ is the diagonal matrix element of the Hamiltonian of the system in the generating coordinate, and it is obtained by:

$$E(S) = \frac{\langle \Psi(S)|H|\Psi(S)\rangle}{\langle \Psi(S)|\Psi(S)\rangle}$$

where $\langle \Psi(S)|H|\Psi(S)\rangle$ and $\langle \Psi(S)|\Psi(S)\rangle$ are the Hamiltonian matrix and the overlap of the state. The $\Psi(S)$ is:

$$\Psi(S) = \mathcal{A} \int \frac{d\Omega_S}{\sqrt{4\pi}} \prod_{\alpha=1}^{2} \phi_\alpha(\mathbf{S}) \prod_{\beta=3}^{4} \phi_\beta(-\mathbf{S}) \times [[\eta_{I_A S_A} \eta_{I_B S_B}]^{I S} Y^L(\hat{\mathbf{S}})]^J [\chi_A^c \chi_B^c]^{[\sigma]}. \quad (30)$$

The results of the three sets of parameters are consistent with each other. To save space, we only show the results of ChQM II here. For the color singlet channels, the effective potentials are shown in Fig. 1, in which we can see that all effective potentials are repulsive. That's why we cannot get any bound state. For the hidden color channel, we gives the potential of ChQM II in Fig. 2. We can see that the minimum potential of each channel appears at the separation of 0.3 or 0.4 fm, which indicates that two colorful subclusters are not willing to huddle together or fall apart, so it is possible to form some resonance states here. However, the energy of the hidden color channel listed in Table 3 is among 4.1–4.6 GeV, which indicates that these resonances may not be suitable to explain the observed $Z_{cs}(3985)^-$ or $Z_{cs}(4000)^+$. The scattering process of the corresponding open channels should be studied to confirm if there is any resonance state or not.

We also try to investigate why the effective potential is repulsive in the color singlet channels. The Hamiltonian of the ChQM consists of mass, the kinetic energy (V_{VK}), the confinement (V_{CON}), the Coulomb interaction (V_{Coul}) and the color-magnetic interaction (V_{CMI}). We take the results of the $IJ^P = \frac{1}{2}0^+$ $\eta_c K^-$ channel in $q\bar{q} - q\bar{q}$ structure as an example. We find that the kinetic energy term in the ChQM provides repulsion. Since there is no exchange items between $c\bar{c}$ and $s\bar{u}$ in ChQM, the confinement, the Coulomb interaction and the color-magnetic interaction do not contribute to the effective potential between two color singlet clusters $c\bar{c}$ and $s\bar{u}$. So the interaction between the two mesons is only affected by the kinetic energy term, which provides repulsive interactions. Therefore, there is no any term which provides attractive interaction between two color singlet clusters in ChQM, which leads to the absence of bound states in this system.

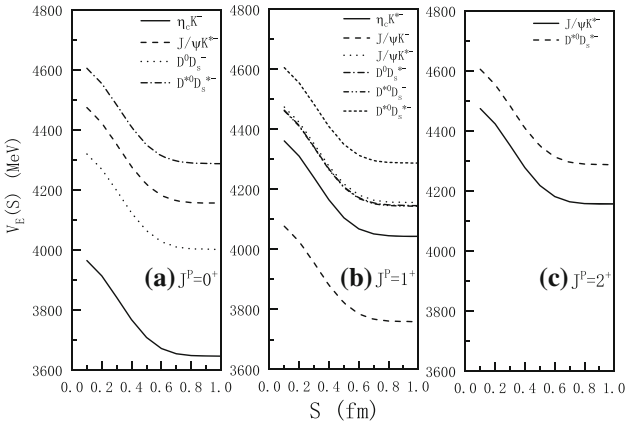

Fig. 1 The effective potentials of the color singlet channels for the $q\bar{q} - q\bar{q}$ systems in the ChQM II

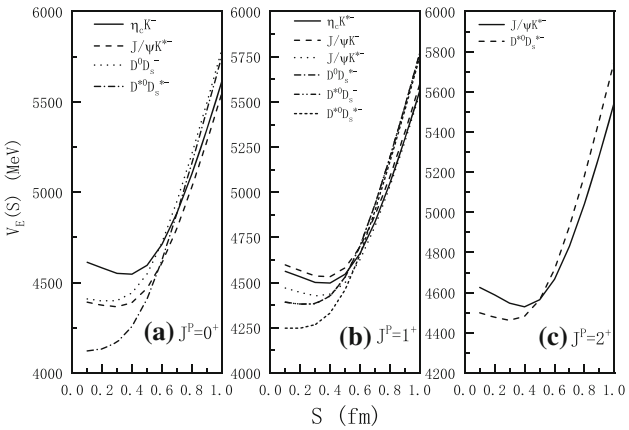

Fig. 2 The effective potentials of the hidden-color channels for the $q\bar{q} - q\bar{q}$ systems in the ChQM II

3.2 $qq - \bar{q}\bar{q}$ structure

With regards to the $qq - \bar{q}\bar{q}$ structure, the results of three sets of parameters in ChQM are listed in Table 4. As shown in the table, the $qq - \bar{q}\bar{q}$ structure has higher energy than the $q\bar{q} - q\bar{q}$ structure so there is no any bound state. We also find that the channel coupling of the $qq - \bar{q}\bar{q}$ structure can make the energy lower, but the energy of each state is still higher than the corresponding threshold. However, since the confinement potential requires that the colorful subclusters diquark and antidiquark cannot fall apart directly, resonance states are possible in this configuration. We perform an adiabatic calculation to check the possibility of the existence of any resonance state, the results of which are shown in Fig. 3.

Obviously, the energy of each single channel will rise when the two subclusters are too close, so there is a hinderance for the state changing structure to $q\bar{q} - q\bar{q}$ even if

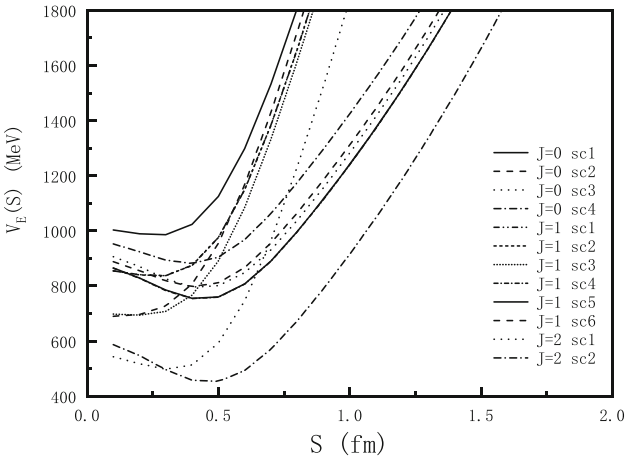

Fig. 3 The effective potentials for the $qq-\bar{q}\bar{q}$ systems in the ChQM II

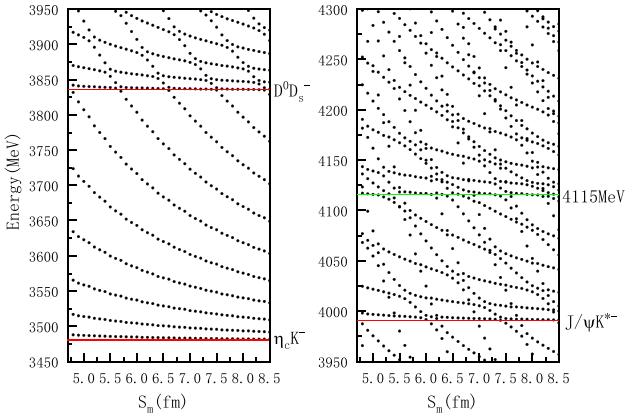

Fig. 4 The stabilization plots of the energies of the $cs\bar{c}\bar{u}$ system with $IJ^P = \frac{1}{2}0^+$ in the ChQM II

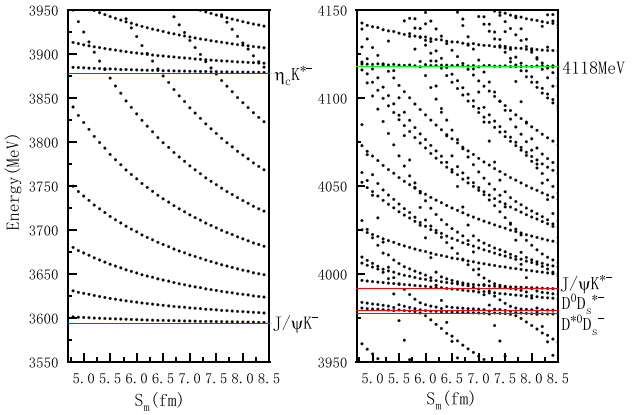

Fig. 5 The stabilization plots of the energies of the $cs\bar{c}\bar{u}$ system with $IJ^P = \frac{1}{2}1^+$ in the ChQM II

the energy of the $qq-\bar{q}\bar{q}$ state is higher than the $q\bar{q}-q\bar{q}$ state. So it is possible to form a resonance state. The minimum energy of each channel appears at the separation of 0.3–0.4 fm, which indicates that the diquark and antidiquark subclusters are close to each other in the ChQM. Therefore, the resonance state may be the compact resonance state. According to the Table 4, after the channel coupling calculation, the lowest resonance energies are 3950.6–4006.0 MeV for $IJ^P = \frac{1}{2}0^+$, 4058.1–4125.4 MeV for $IJ^P = \frac{1}{2}1^+$, and 4411.1–4423.5 MeV for $IJ^P = \frac{1}{2}2^+$. Although the energy of the $IJ^P = \frac{1}{2}0^+$ state is close to the reported $Z_{cs}(3985)^-$ or $Z_{cs}(4000)^+$, the existence of these resonance states should be checked by coupling to the corresponding open channels. Because the coupling to the open channels will shift the mass of the resonance and give the decay width to the resonance, or destroy the resonance. So we couple all the channels with both the $q\bar{q}-q\bar{q}$ and the $qq-\bar{q}\bar{q}$ structures to confirm if there is any resonance state.

3.3 Two structures coupling

In this section, a stabilization method [44], which is effective in the study of electron–atom, electron–molecule and atom–diatom complexes, is used to find the genuine resonance states. This method was also called as the real scaling method, which has been employed to the pentaquark systems within the quark model calculation [45,46]. Besides, we also applied this method to find several resonance states of the fully heavy tetraquark systems and found that the reported state $X(6900)$ can be explained as a compact resonance state with $IJ^P = 00^+$ [38]. Therefore, extending to the tetraquark system composed of $cs\bar{c}\bar{u}$ is feasible. Moreover, a channel-coupling calculation of all channels with both $q\bar{q}-q\bar{q}$ and $qq-\bar{q}\bar{q}$ configurations is carried out here. In our calculation, the distance between two clusters is denoted by S_i, and the maximum one is S_m. We increase S_m from 4.8 to 8.5 fm to observe the change of the energy of the $cs\bar{c}\bar{u}$ system. If the eigenvalue decreases and eventually approaches to the threshold, it means that this is an unbound state, while if the energy tends to be stable, it indicates that this is a resonance state. The stabilization plots of the energies of the $cs\bar{c}\bar{u}$ systems in the ChQM II with possible quantum numbers are shown in Figs. 4, 5 and 6.

Figure 4 shows the results of the $cs\bar{c}\bar{u}$ systems with $IJ^P = \frac{1}{2}0^+$ in the ChQM II. There are three red horizontal lines, which represent the thresholds of $\eta_c K^-$, $D^0 D_s^-$ and $J/\psi K^{*-}$, respectively. Another horizontal line around 4115 MeV is stable with the variation of the distance between two clusters, so it is on behalf of a resonance state. Besides, we also calculate the component of each channel for this resonance state, and find that the main ingredient is $D^{*0}D_s^{*-}$. So by considering the effect of all channels coupling, the former resonance state around 3964.6 MeV with $qq-\bar{q}\bar{q}$ configuration disappears. Instead, a new resonance state $D^{*0}D_s^{*-}$ around the energy 4115 MeV is obtained.

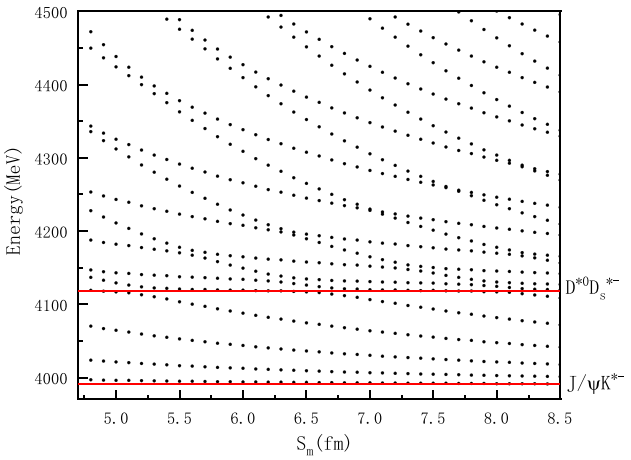

Fig. 6 The stabilization plots of the energies of the $cs\bar{c}\bar{u}$ system with $IJ^P = \frac{1}{2}2^+$ in the ChQM II

For the $cs\bar{c}\bar{u}$ systems with $IJ^P = \frac{1}{2}1^+$, the first five horizontal lines stand for the thresholds of channels $J/\psi K^-$, $\eta_c K^{*-}$, $D^{*0}D_s^-$, $D^0 D_s^{*-}$ and $J/\psi K^{*-}$, respectively. Another horizontal line around 4118 MeV is stable as the distance between two clusters increasing, which indicates that there is a resonance state around the energy of 4118 MeV. Moreover, the main component of this state is $D^{*0}D_s^{*-}$, too.

The results of the $cs\bar{c}\bar{u}$ systems with $IJ^P = \frac{1}{2}2^+$ are shown in Fig. 6. It is obvious that the first two horizontal lines represent the thresholds of $J/\psi K^{*-}$ and $D^{*0}D_s^{*-}$. However, no any resonance state is found here.

Besides, we also find that the results of the three sets of parameters are consistent with each other. By taking into account the effect of the channel-coupling, the resonance state around 3964.6 MeV disappears. We cannot find any resonance states that could explain the reported $Z_{cs}(3985)^-$ or $Z_{cs}(4000)^+$ at present. However, we find two new resonance states, which are $IJ^P = \frac{1}{2}0^+$ state with energy around 4111–4116 MeV and $IJ^P = \frac{1}{2}1^+$ state with resonance energy around 4113–4119 MeV, respectively. The main component of these two resonant states is $D^{*0}D_s^{*-}$. This conclusion is consistent with that of many theoretical studies [14,20,26,28,29], in which the new exotic state with energy around 4120 MeV is predicated. We suggest that experiments can verify the existence of these resonance states.

4 Summary

In this work, we systematically investigate the low-lying charged hidden-charm tetraquark systems with strangeness in the ChQM with three different sets of parameters. Two configurations, $q\bar{q} - q\bar{q}$ and $qq - \bar{q}\bar{q}$, as well as the coupling of these two structures are considered. The dynamical bound-state calculation is carried out to search for any bound state in the $cs\bar{c}\bar{u}$ systems. To investigate the effect of the channel coupling, both the single channel and the channel coupling calculation are performed. Meanwhile, an adiabatic calculation of the effective potentials is added to study the interactions of the systems and a stabilization calculation is carried out to find any resonance state.

The bound-state calculation shows that there is no any bound state in ChQM, which excludes the molecular state explanation ($D^0 D_s^{*-}/D^{*0}D_s^-/D^{*0}D_s^{*-}$) of the reported $Z_{cs}(3985)^-$ or $Z_{cs}(4000)^+$. The study of the interaction between two mesons shows that the confinement interaction, the Coulomb interaction and the color-magnetic interaction don't work between two mesons of the $cs\bar{c}\bar{u}$ systems, because there is no exchange items between them. So it is difficult to obtain a molecular state in this $cs\bar{c}\bar{u}$ system in present work. However, the effective potentials for the $cs\bar{c}\bar{u}$ systems of the $qq - \bar{q}\bar{q}$ configuration shows the possibility of some resonance states. Although we can obtain a resonance state of the $qq - \bar{q}\bar{q}$ structure with $IJ^P = \frac{1}{2}0^+$, the energy of which is 3964.6 MeV, closing to the $Z_{cs}(3985)^-$, it disappears by coupling all channels of both $q\bar{q} - q\bar{q}$ and $qq - \bar{q}\bar{q}$ structures. Nevertheless, two new resonance states are obtained, which are the $IJ^P = \frac{1}{2}0^+$ state with energy around 4111–4116 MeV and the $IJ^P = \frac{1}{2}1^+$ state with resonance energy around 4113–4119 MeV, respectively. Both of them are worth searching by experiments.

Up to now, none of the exotic hadron states is definitely confirmed by experiment. To each experimental observation, there always exists many different theoretical interpretations. To provide the necessary information for experiments to search for exotic hadron states, the coupling calculation between the bound channels and open channels is indispensable. The stabilization method is one of the effective ways to look for the genuine resonances. Besides, the study of the scattering process of the corresponding open channels is also an efficient way, which is our further work. However, to distinguish the various explanations and confirm the existence of the exotic hadron states is still very difficult, which requires the joint efforts of both theorists and experimentalists.

Acknowledgements This work is supported partly by the National Science Foundation of China under Contract nos. 11675080, 11775118 and 11535005, and the Joint Large-Scale Scientific Facility Funds of the National Natural Science Foundation of China NSFC and the Chinese Academy of Sciences CAS under Contract no. U1732105.

Data Availability Statement This manuscript has no associated data or the data will not be deposited. [Authors' comment: The data have been illustrated in the figures and tables, so they are not necessary to be deposited. Data may be made available upon request.]

Funded by SCOAP[3].

References

1. M. Ablikim et al. (BESIII), Phys. Rev. Lett. **110**, 252001 (2013)
2. Z.Q. Liu et al. (Belle), Phys. Rev. Lett. **110**, 252002 (2013)
3. Z. Liu, arXiv:1311.0762 [hep-ex]
4. M. Ablikim et al. (BESIII), Phys. Rev. Lett. **111**(24), 242001 (2013)
5. M. Ablikim et al. (BESIII), Phys. Rev. Lett. **112**(13), 132001 (2014)
6. M. Ablikim et al. (BESIII), Phys. Rev. Lett. **112**(2), 022001 (2014)
7. K. Chilikin et al. (Belle), Phys. Rev. D **90**(11), 112009 (2014)
8. M. Ablikim et al. (BESIII), Phys. Rev. Lett. **115**(18), 182002 (2015)
9. M. Ablikim et al. (BESIII), Phys. Rev. Lett. **126**(10), 102001 (2021)
10. J.Z. Wang, Q.S. Zhou, X. Liu, T. Matsuki, Eur. Phys. J. C **81**(1), 51 (2021)
11. L. Meng, B. Wang, S.L. Zhu, Phys. Rev. D **102**(11), 111502 (2020)
12. Z. Yang, X. Cao, F.K. Guo, J. Nieves, M.P. Valderrama, Phys. Rev. D **103**(7), 074029 (2021)
13. R. Chen, Q. Huang, Phys. Rev. D **103**(3), 034008 (2021)
14. M.C. Du, Q. Wang, Q. Zhao, arXiv:2011.09225 [hep-ph]
15. X. Cao, J.P. Dai, Z. Yang, Eur. Phys. J. C **81**(2), 184 (2021)
16. B.D. Wan, C.F. Qiao, Nucl. Phys. B **968**, 115450 (2021)
17. Z.F. Sun, C.W. Xiao, arXiv:2011.09404 [hep-ph]
18. G.C. Rossi, G. Veneziano, Nucl. Part. Phys. Proc. **312–317**, 140–145 (2021)
19. Q.N. Wang, W. Chen, H.X. Chen, Chin. Phys. C **45**(9), 093102 (2021)
20. B. Wang, L. Meng, S.L. Zhu, Phys. Rev. D **103**(2), L021501 (2021)
21. Z.G. Wang, Chin. Phys. C **45**(7), 073107 (2021)
22. K. Azizi, N. Er, Eur. Phys. J. C **81**(1), 61 (2021)
23. Y.A. Simonov, JHEP **04**, 051 (2021)
24. M.J. Yan, F.Z. Peng, M. Sánchez Sánchez, M. Pavon Valderrama, arXiv:2102.13058 [hep-ph]
25. R. Aaij et al. (LHCb), Phys. Rev. Lett. **127**(8), 082001 (2021)
26. P.G. Ortega, D.R. Entem, F. Fernandez, Phys. Lett. B **818**, 136382 (2021)
27. J.F. Giron, R.F. Lebed, S.R. Martinez, Phys. Rev. D **104**(5), 054001 (2021)
28. P.P. Shi, F. Huang, W.L. Wang, Phys. Rev. D **103**(9), 094038 (2021)
29. L. Meng, B. Wang, G.J. Wang, S.L. Zhu, Sci. Bull. **66**, 2065–2071 (2021)
30. H.X. Chen, arXiv:2103.08586 [hep-ph]
31. S.H. Lee, M. Nielsen, U. Wiedner, J. Korean Phys. Soc. **55**, 424 (2009)
32. M.B. Voloshin, Phys. Lett. B **798**, 135022 (2019)
33. J. Ferretti, E. Santopinto, JHEP **04**, 119 (2020)
34. D. Ebert, R.N. Faustov, V.O. Galkin, Phys. Lett. B **634**, 214–219 (2006)
35. D.Y. Chen, X. Liu, T. Matsuki, Phys. Rev. Lett. **110**, 232001 (2013)
36. C. Deng, J. Ping, F. Wang, Phys. Rev. D **90**, 054009 (2014)
37. A. Valcarce, H. Garcilazo, F. Fernández, P. Gonzalez, Rep. Prog. Phys. **68**, 965 (2005)
38. X. Jin, Y. Xue, H. Huang, J. Ping, Eur. Phys. J. C **80**(11), 1083 (2020)
39. R. Aaij et al. (LHCb), Sci. Bull. **65**(23), 1983–1993 (2020)
40. J. Vijande, F. Fernandez, A. Valcarce, J. Phys. G **31**, 481 (2005)
41. M. Kamimura, Suppl. Prog. Theor. Phys. **62**, 236 (1977)
42. A.J. Buchmann, Y. Yamauchi, A. Faessler, Nucl. Phys. A **496**, 621 (1989)
43. Y. Tan, W. Lu, J. Ping, Eur. Phys. J. Plus **135**, 716 (2020)
44. J. Simon, J. Chem. Phys. **75**, 2465 (1981)
45. E. Hiyama, M. Kamimura, A. Hosaka, H. Toki, M. Yahiro, Phys. Lett. B **633**, 237–244 (2006)
46. E. Hiyama, A. Hosaka, M. Oka, J.M. Richard, Phys. Rev. C **98**(4), 045208 (2018)